HHS Public Access

Author manuscript

Neurobiol Aging. Author manuscript; available in PMC 2016 May 01.

Published in final edited form as:

Neurobiol Aging. 2015 May ; 36(5): 1982–1993. doi:10.1016/j.neurobiolaging.2015.02.006.

Age-related changes in Regulator of G-protein Signaling (RGS)-10 expression in peripheral and central immune cells may influence risk for age-related degeneration

George T. Kannarkat[1], **Jae-Kyung Lee**[1,#], **Chenere P. Ramsey**[1], **Jaegwon Chung**[1], **Jianjun Chang**[1], **Isadora Porter**[1], **Danielle Oliver**[1], **Kennie Shepherd**[2], and **Malú G. Tansey**[1,#]

[1]Department of Physiology, Emory University School of Medicine, Atlanta, Georgia 30322

[2]Department of Pharmacology and Toxicology, Morehouse School of Medicine, Atlanta, GA

Abstract

Inflammation in the aging brain increases risk for neurodegenerative disease. In humans, the Regulator of G-protein Signaling (RGS) 10 locus has been associated with age-related maculopathy. Chronic peripheral administration of lipopolysaccharide in the RGS10-null mice induces nigral dopaminergic (DA) degeneration, suggesting that RGS10 modulates neuroimmune interactions and may influence susceptibility to neurodegeneration. Since age is the strongest risk factor for neurodegenerative disease, we assessed whether RGS10 expression changes with age and whether aged RGS10-null mice have altered immune cell profiles. Loss of RGS10 in aged mice does not alter the regulation of nigral DA neurons but does alter B cell, monocyte, microglial and CD4+ T cell populations and inflammatory cytokine levels in the cerebrospinal fluid. These results suggest that loss of RGS10 is associated with an age-dependent dysregulation of peripheral and central immune cells rather than dysregulation of dopaminergic neuron function.

Keyword word list

RGS10; immune cells; aging; midbrain; dopamine; tyrosine hydroxylase; oxidative stress

1. Introduction

Aging is the largest risk factor for neurodegenerative diseases such as age-related maculopathy and Parkinson's disease (Hindle, 2010, van Lookeren Campagne, et al., 2014). The convergence of multiple mechanisms accounts for this risk: protein aggregation,

[#]Co-corresponding Authors: Malú G. Tansey, Ph.D., Department of Physiology, Emory University School of Medicine, 615 Michael Street, 605L Whitehead Biomedical Research Bldg., Atlanta, GA 30322, USA. malu.tansey@emory.edu. Jae-Kyung Lee, Ph.D., Department of Physiology, Emory University School of Medicine, 615 Michael Street, 605K Whitehead Biomedical Research Bldg., Atlanta, GA 30322, USA. jaekyung.lee@emory.edu.

Disclosures: The authors report no real or potential conflicts of interest.

mitochondrial dysfunction, oxidative stress, and inflammation (Reitz and Mayeux, 2014, Tansey and Goldberg, 2010). The role of the Regulator of G Protein Signaling (RGS) 10 in modulating interactions between the immune and nervous systems makes it an interesting target to study in the context of aging (Pankratz, et al., 2003). The locus encoding the RGS10 protein on chromosome 10q26 has been associated with age-related maculopathy, a disease of retinal degeneration with significant microgliosis (Jakobsdottir, et al., 2005, Schmidt, et al., 2006). A polymorphism in *RGS10* has also been associated with schizophrenia (Hishimoto, et al., 2004). Given these associations in humans, it is particularly interesting that the global loss of RGS10 in the mouse leads to microgliosis and susceptibility to degeneration of DA neurons in the midbrain in response to peripheral low dose administration of lipopolysaccharide (Lee, et al., 2011, Lee, et al., 2008). This unique phenotype implicates RGS10 as a potential regulator of neuroimmune interactions and raises the question of its role in aging.

RGS10, the smallest of the RGS proteins, belongs to the R12 subfamily and is highly expressed in the brain, thymus, and lymph nodes (Gold, et al., 1997, Hunt, et al., 1996, Ross and Wilkie, 2000, Sierra, et al., 2002). The physiologic substrates of RGS10 have not been identified, but in heterologous assays it is known to selectively accelerate the GTPase activity of $G\alpha_{i3,}$ $G\alpha_{q,}$ $G\alpha_{z}$ (Hunt, et al., 1996). Aging has been shown to affect the repertoire and function of G-protein coupled receptors (GPCRs) and proteins (Alemany, et al., 2007). GPCRs are involved in controlling critical cellular and physiological functions. GPCRs signal through heterotrimeric G-proteins that consist of α subunit and βγ heterodimer (Joseph, et al., 1993, Neves, et al., 2002). RGS proteins contain an evolutionarily conserved RGS domain that interacts with $G\alpha_{i}$, $G\alpha_{q/11}$, $G\alpha_{12/13}$ or Gαs subunits with variable selectivity, to accelerate intrinsic GTPase activating function of the Gα subunits therein (Berman, et al., 1996, Ross and Wilkie, 2000, Siderovski, et al., 1999). Age-associated changes in GPCRs and G-proteins vary throughout the body but the expression of most GPCRs and G-proteins decrease with age in the brain (Joseph, et al., 1993, Mato and Pazos, 2004, Pascual, et al., 1991, Sastre, et al., 2001). In human lymphocytes and neutrophils, there were a variety of changes in the pattern and the quantity of G proteins with aging (Fulop, et al., 1992). It has been also reported that Gα subunits may undergo age-related changes that impair coupling to G-proteins after agonist-binding. This impaired coupling would decrease the proportion of high affinity receptors that could be formed (Alemany, et al., 2007). In turn, age-related changes in G-protein signaling could help explain dyregulation in numerous physiologic and cellular systems that occur with aging.

In addition to human disease associations and the sensitivity of nigral DA neurons to LPS-induced degeneration, previous work from our group and others have implicated RGS10 in immune cell and neuronal function. Specifically, we reported that RGS10 negatively regulates Nuclear Factor-κ-light-chain-enhancer of activated B cells (NF-κB) signaling, explaining the pro-inflammatory phenotype of RGS10-null microglia (Lee, et al., 2011). In dopaminergic (DA) neurons, RGS10 plays a neuroprotective role through interactions with the Protein Kinase A (PKA)/cAMP response element-binding protein (CREB) pathway (Lee, et al., 2012). We also demonstrated that loss of RGS10 induces a dysregulated phenotype in peripheral macrophages (Lee, et al., 2013). RGS10 has also been implicated as

a negative regulator of chemokine-dependent adhesion via the Vav1-Rac1-dependent pathway (Garcia-Bernal, et al., 2011). In platelets, RGS10 binds to Src homology 2 domain-containing phosphatase 1 (SHP-1) and negatively regulates platelet activation through a sphinophilin-dependent pathway (Ma, et al., 2012). The SHP-1 pathway is also very important in immune cells as a negative regulator of activation. The role of RGS10 in modulating these pathways could provide an explanation for the neurodegeneration seen in RGS10-null mice after chronic peripheral LPS administration. Given that age is the strongest risk factor for neurodegeneration and that RGS10 plays a role in modulating many pathways involved in neuroimmune interactions, we hypothesized that RGS10 would play an important role in altering the regulation of DA neurons and immune cell populations in aging.

2. Materials and methods

2.1 Animals

Generation of RGS10-null mice (C57/B6) has been described previously (Lee, et al., 2011). Three to seven month old (young) mice and 18–22 month old (aged) mice were used for experiments. Age- and gender- matched wild-type (WT) mice were used as controls. Experimental procedures involving use of animal tissue were performed in accordance with the NIH Guidelines for Animal Care and Use and approved by the Institutional Animal Care and Use Committee at Emory University School of Medicine in Atlanta, GA. Unless noted, mice were euthanized by intraperitoneal Euthasol injection.

2.2 Flow Cytometry

From mice, spleens were homogenized into a single-cell suspension and blood was collected in EDTA-coated tubes by cheek bleed and then red blood cells (RBCs) were lysed with RBC lysis buffer (1.5M NH_4Cl, 0.1 M $KHCO_3$, Na_2EDTA, pH 7.4) For surface staining, cells were washed with FACS buffer and then stained for 20 minutes with fluorophore-conjugated antibodies. For mouse tissues, the antibodies used wereanti-CD11b-PE (ebiosciences), anti-Ly6G-FITC (ebiosciences), anti-CD45-APC (ebiosciences), anti-CD3ε-PE-Cy7 (ebiosciences), anti-CD8α-APC-Cy7 (ebiosciences), anti-CD4-V500 (BD Biosciences) and anti-CD16/CD32 (ebiosciences). If applicable, intracellular staining was then performed using Invitrogen Fixation and Permeabilization Media with goat anti-RGS10 primary antibody (Santa Cruz Biotechnology) and donkey anti-goat Fc FITC-conjugated secondary antibody (Santa Cruz Biotechnology). If intracellular staining was not performed, cells were washed and then fixed with 1% paraformaldehyde for 30 minutes. After washing, cells were stored in FACS buffer until analysis on a LSR-II flow cytometer (BD Biosciences). Data analysis was performed on FlowJo software.

2.3 Immunofluorescence and Image Quantitation

Mice were anesthetized with 200 mg/kg Euthasol (Virbac Animal Health, Fort Worth, TX) and brains extracted and fixed for 24 hours in 4% paraformaldehyde. Brains were sectioned onto glass slides (Leica Cryostat CM3050 S). Sections on glass slides were fixed for an additional 15 min in 4 % paraformaldehyde, followed by a 1 X PBS rinse, pH 7.4. Sections were incubated in 0.2 M glycine, pH 7.4, for 30 min to minimize tissue autofluorescence

caused by the aldehyde fixative. Sections were permeabilized for 35 min in Tris-buffered saline (TBS) containing 0.3 % Triton X-100 and 1 % normal donkey serum (NDS), followed by blocking for 60 min in TBS containing 1 % NDS. Sections were incubated in primary antibody for 24 hrs at 4 °C in TBS containing 0.1 % Triton X-100 and 1 % NGS. Iba1 (Wako Pure Chemical Industries, Ltd., Osaka, Japan) (1:250), RGS10 (C-20, Santa Cruz) (1:200) followed by the appropriate Alexa-conjugated secondary antibodies (1:500, Invitrogen). Non-immune IgG sera at the same concentration as the primary antibodies were used to confirm the specificity of staining. To quantify the level of RGS10 on Iba1+ cells, 5–6 sections per animal from young and aged wild-type mice (n=3) were selected between bregma −1.28 mm and −2.12 mm. Images of RGS10+ or Iba1+ cells from 20 random fields of brain sections were captured under 20x objective lens on a Nikon 90i fluorescence microscope using thresholding analysis on Nikon Elements 5 software. RGS10 expression in Iba1+ cells was quantified in these images using ImageJ software. Total RGS10 expression intensity in fields was quantified by thresholding on the mean intensity value + 80 intensity units of Iba1 fluorescence intensity. The average RGS10 expression intensity and average number of RGS10-immunoreactive pixels per Iba1+ cell was quantified after thresholding on the mean intensity value + 80 intensity units of Iba1 fluorescence intensity and then using the Analyze Particles function.

2.4 Cerebrospinal fluid (CSF) and Serum collection

Mice were anesthetized with mixtures of Ketamine (100 mg/kg), Xylazine (10 mg/kg) and Acepromazine (2 mg/kg) and placed into a stereotaxic frame with the nose pointed down. Then, a small gauge needle was inserted into the cisterna magna (the triangular space between the back of the cerebellum and the medulla oblangata). A silastic tube was attached to the needle to drain CSF into a test tube. CSF was visually checked for blood contamination and not used in analysis if fluid was opaque, cloudy, or colored. Blood was collected into EDTA-coated tubes by the cheek bleed method using a lancet to puncture the submandibular vein. Serum was separated from blood samples using Microvettes® 200 Z-Gel (SARSTEDT) by centrifugation at 10,000 rpm for 5 min at room temperature.

2.5 Multiplexed ELISAs

Serum and CSF were analyzed for cytokines and chemokines (mouse IFN-γ, IL-1β, IL-6, IL-10, IL-12, KC, and TNF) using a multiplexed immunoassay per the manufacturer's instructions (Meso-Scale Discovery, Gaithersburg, MD).

2.6 Immune Cell Isolation from Adult Mouse Brain

Microglia were isolated from adult mice as described previously (Lee and Tansey, 2013). Briefly, brain was finely minced using a scalpel and digested using a papain-dispase solution at 37°C. Microglia and other immune cells were separated from myelin, red blood cells, and other cell debris by collecting the 30:37 layer interface of a 30:37:70 Percoll gradient. Immune cells were washed out from Percoll with 1x Hank's Balanced Salt Solution by density centrifugation.

2.7 Western blot analysis

Striatum and/or ventral midbrain tissues were dissected from RGS10 WT or null animals. Tissues were sonicated in 2% SDS/8M Urea. Total protein extracts were then quantified using the bicinchoninic acid (BCA) assay (Pierce Biotechnology, Rockford, IL, USA) and bovine serum albumin as the standard. Equal amounts of protein extracts were resolved by SDS–PAGE and analyzed by immunoblot using rabbit polyclonal Anti-Tyrosine Hydroxylase Antibody (AB152; Millipore), mouse monoclonal α-tubulin antibody (Calbiochem), and goat polyclonal RGS10 (C-20) antibody (Santa Cruz Biotechnology). Images were quantified using GeneTools image analysis software (Syngene).

2.8 Quantitative Real-time RT-PCR (QPCR)

Striatum and/or ventral midbrain tissues were dissected from RGS10 wild-type (WT) or RGS10 null animals and frozen on dry ice. Total RNA was extracted using TRIzol reagent (Invitrogen) and purified using the RNeasy Mini Kit (Qiagen) according to the manufacturer's instructions. Up to 2 ug of each RNA sample was treated with DNase I and reverse transcribed with SuperScript II Reverse Transcriptase (Invitrogen) according to the manufacturer's protocol. QPCR was performed using Power SYBR Green PCR Master Mix (Applied Biosystems) and previously validated QPCR primers for murine GAPDH (forward: 5′CAAGGTCATCCATGACAACTTTG3′; reverse: 5′GGCCATCCACAGTCTTCTGG3′), Nrf2 (forward: 5′CCCGGTTGCCCACATTC3′; reverse: 5′TGTCTCTGCCAAAAGCTGCAT3′), Parkin (forward: 5′AGCCCTCCAAGGAAACCATC3′; reverse: 5′CGTTTTTTTCAATTGGCACGT3′), and TH (forward: 5′TTGGCTGACCGCACATTT3′; reverse: 5′GCCCCCAGAGATGCAAGT3′) genes. Reactions were performed in triplicate using an ABI Prism 7900HT Sequence Detection System (Applied Biosystems) and data were analyzed by the ΔΔ Ct method.

2.9 Dopamine Metabolism Measurement

Neurochemical analysis was performed as previously described (Shepherd, et al., 2006) with slight modifications. Briefly, mice (n = 4 per age group) were sacrificed and the brain was placed in a mouse brain matrix (Asi-Instruments). Coronal sections (2 mm) of the brain were cut by placing razor blades in each channel in the matrix. The coronal sections containing the striatum were placed on a cooled plate, and the striatum was dissected out. Tissue was weighed and homogenized in 10 volumes of ice-cooled 0.1 M perchloric acid (containing 347 μM sodium metabisulfate, 134 μM EDTA,) and then centrifuged at 4 °C for 15 min at 10,000×g. The supernatants were filtered using 0.2 μm filters (Fisher) for 2 min at 10,000×g. Dopamine (DA), and its metabolites 3–4-dihydroxphenylacetic acid (DOPAC) and homovanillic acid (HVA), and 3-methoxytyramine (3-MT) were analyzed using reverse-phase ion pairing ultra-high pressure liquid chromatography (UHPLC, Dionex-ThermoFisher) combined with a electrochemical (EC) detector (Coulochem III, ESA) under isocratic conditions (Shepherd et al., 2006). The guard cell was set at +350 mV, with a screening electrode set at −150 mV, and working electrode set at +220 mV. The mobile phase consisted of 75 mM sodium dihydrogen phosphate monohydrate, 1.7 mM 1-octane sulfonic acid sodium salt, 0.73 mM triethylamine, 25 μM EDTA, 10 % acetonitrile/90 %

water. The pH was adjusted to 3.0 with phosphoric acid. The mobile phase was delivered at a flow rate of 0.6 ml/min onto the MD-150 (3 × 150 mm, 3 μm) reverse phase column (ESA, Chelmsford, MA, USA). Twenty microliters aliquots were injected by an autoinjector with cooling module set at 4 °C. The levels of DA, DOPAC, HVA, 3-MT in unknown samples were determined using standard curves created by injection of known concentrations of each compound.

2.9 Statistical analysis

Comparison among more than two groups for experiments was analyzed by two-way ANOVA followed by the Bonferroni *post-hoc* test for *p* values. Comparison between just two groups was tested by the two-tailed Student's t-test. Specific stastitical tests and number of animals used in each group for every experiment are indicated in figure legends.

3. Results

RGS10 expression in B cells, monocytes, and granulocytes is increased with age while microglial RG10 expression decreases

To assess whether RGS10 expression is important for regulation of immune cell subsets with aging, we first measured the level of expression in various immune cell subsets from the peripheral blood and spleen (Fig 1). In the peripheral blood, RGS10 expression significantly increases with age in CD19+CD45+ B cells, CD19-CD3-CD45+CD11b+Ly6G − monocytes, and CD19-CD3-CD45+CD11b+Ly6G+ granulocytes (Fig 1A). RGS10 expression did not increase with age in CD45+CD3+ T cells. In splenocytes, RGS10 expression significantly increases with age in monocytes, macrophages and granulocytes (Fig 1B). Then, we also quantified the RGS10 expression in Iba1+ cells in the brain by immunofluorescent staining demonstrating that the total level of RGS10 expression in Iba1+ cells, average level of RGS10 expression per Iba1+ cell, and average area of RGS10+ immunoreactivity per Iba1+ cell was decreased in aged mice (Fig 1C). Representative images of Iba1 and RGS10 staining visually confirm similar findings to quantification (Fig 1D). In summary, RGS10 expression in mice increases in B cells, monocytes, and granulocytes but decreases in Iba1+ cells in the brain with aging.

Loss of RGS10 has minimal effect on frequency and number of peripheral immune cell subsets but does alter immune cell frequencies in the brain in young mice

To investigate whether loss of RGS10 alters the profile of immune cell subsets, we determined the frequency and number of immune cell subsets in the peripheral blood and spleen as well as the brain. There was a slight yet a significant decrease in the frequency of CD8+ splenocytes in RGS10-null mice (Fig 2A, 2B). The frequency and number of other immune cell subsets in the periphery remained unchanged by loss of RGS10. In the brains of young RGS10-null mice, the frequency of monocytes/microglia was decreased while the frequency of granulocytes and CD8+ T cells was increased. In addition, the number of granulocytes in the brains of young RGS10-null was increased. Therefore, we see alterations in the immune cell repertoire of the brains of RGS10-null young mice while the peripheral immune cell repertoire is not significantly altered.

Loss of RGS10 alters B cell, M0, and CD4+ T cell frequency and number in the periphery of but not in the brains of aged mice

Since RGS10 expression increases with age in B cells, monocytes, and granulocytes, we predicted that the homeostatic frequencies of these cell types would be altered in aged RGS10-null mice. Indeed in aged RGS10-null mice, the frequency of B cells and CD4+ T cells in the peripheral blood was significantly decreased while the frequency of monocytes was significantly increased (Fig 3). Furthermore, the absolute number of monocytes and CD4+ T cells in spleens of aged RGS10-null mice was decreased. In summary, the frequency and number of monocytes, B cells, and CD4+ T cells in the periphery but not in the brain was altered by the loss of RGS10 in aged mice.

Loss of RGS10 does not alter serum cytokine levels, but is associated with loss of age-related increase in levels of IL-6 in the cerebrospinal fluid

Since loss of RGS10 in the context of aging altered the homeostatic frequency and number of immune cell subsets, we investigated whether loss of RGS10 altered serum or CSF cytokine or chemokine levels in this same context. Serum and cerebrospinal fluid from WT and RGS10-null mice were collected and analyzed by Multiplex ELISA. There were no major differences in pro-inflammatory cytokine levels in young versus aged mice (Fig 4). The level of the chemokine, KC (CXCL1), increases with age but there is no difference between the genotypes. CSF was pooled within groups and analyzed on a multiplex ELISA. IL-6 level was increased by aging in WT mice but not in RGS10-null mice. Level of TNF-α was increased with age in both genotypes in CSF. The levels of other cytokines in the multiplex ELISA were undetectable in the CSF in all groups. In summary, loss of RGS10 alters the dynamics of IL-6 in the CSF of mice but does not affect the levels of serum cytokines.

RGS10 and Tyrosine Hydroxylase protein expression does not change with age in the ventral midbrain or striatum

Using midbrain dopaminergic cell lines in culture, we previously showed that in response to acute inflammatory insult, RGS10 levels were dramatically diminished (Lee, et al., 2008); however, it is unknown whether the events that occur during aging modulate RGS10 in nigrostriatal brain regions *in vivo*. To determine this, we measured RGS10 steady-state levels in ventral midbrain and striatum tissues from young and aged RGS10 WT mice. It was discovered that RGS10 protein levels were not altered with age in neither ventral midbrain nor striatum tissues (Fig 5A). Next, to determine whether RGS10 is required for normal nigrostriatal DA neuron function in aging, we measured protein levels of the catecholamine neuron marker, tyrosine hydroxylase (TH), in young and aged RGS10 WT and null animals (Fig 5B, C). Interestingly, no differences in TH levels were noted in ventral midbrain tissues when comparing between RGS10 WT and null animals in young or aged groups (Fig 5B, C). This finding suggests that RGS10 gene ablation spares nigrostriatal DA neurons, even during aging.

Loss of RGS10 does not alter tyrosine hydroxylase, Parkin, or Nrf2 mRNA expression in the ventral midbrain in young or aged mice

In efforts to confirm that aging does not alter the expression of RGS10 in nigrostriatal brain regions, RGS10 mRNA levels were quantified in young and aged animal cohorts using QPCR. As expected, no significant differences were noted when comparing RGS10 mRNA levels in RGS10 WT young and aged animal ventral midbrain or striatum tissues (Fig 6A). Further, also consistent with the observations made on the protein level, RGS10 gene ablation did not alter TH mRNA levels in mice, nor did advancing age (Fig 6B).

Next, since we have previously shown deficits in the Parkinson's disease implicated gene product, parkin, to be causal of inflammation-related dopaminergic neuron toxicity (Frank-Cannon, et al., 2008), it was of interest to determine whether RGS10 may be implicated in this pathway. Thus, we measured mRNA levels of parkin in young and aged RGS10 WT and null animal ventral midbrain tissues. However, significant differences in the levels of parkin mRNA were not observed when comparing between any of the animal groups (Fig 6B).

It was also considered that inflammation is often correlated with an increased incidence of oxidative stress. Thus, it was hypothesized that if RGS10 acts to diminish neuroinflammation in DA neurons by modulating the effects of harmful oxidation. To begin to address this hypothesis, expression levels of the well-characterized antioxidant stress response transcription factor, Nuclear factor (erythroid-derived 2)-like 2 (Nrf2), were compared in young and aged RGS10 WT and null animal ventral midbrain tissues. Interestingly, alterations in Nrf2 mRNA levels were not detected when comparing between any of the animal groups (Fig 6B). Together, this evidence indicates that the ablation of RGS10 alone may not be sufficient to induce deleterious effects in dopaminergic neurons, even during aging.

Loss of RGS10 does not alter dopamine metabolism in the nigrostriatal pathway

Although it was observed that TH levels were not modulated by ablation of RGS10 in animals, it was of interest to determine whether loss of RGS10 alters the function of dopaminergic neurons in the nigrostriatal pathway. To assess this, striatal tissues from young and aged RGS10 WT and null animals were analyzed for the levels of DA and its metabolites using HPLC with electrochemical detection. Although no differences in the levels of DA were observed when comparing between any of the animal groups (Fig 7), interestingly, it was discovered that the degradation rate of DA in presynaptic dopaminergic neuron terminals was significantly decreased with age in RGS10 WT mice, as indicated by a ~1.25 fold lower ratio of striatal 3–4-dihydroxphenyl-acetic acid (DOPAC)/DA levels in comparison to the young RGS10 WT group. This effect was not seen in the RGS10-null mice (Fig 7B, left panel). Notwithstanding, it is worth noting that young RGS10-null mice exhibited a trend towards diminished striatal DOPAC levels in comparison to the young RGS10 WT mouse group, though the results were not significant (data not shown). No significant differences in the ratios of homovanillic acid (HVA)/DA levels or 3-methoxytyramine (3-MT)/DA levels were observed when comparing between any of the

mouse groups, suggesting that neither age nor loss of RGS10 significantly alter DA degradation that occurs in extranigral cell types.

4. Discussion

RGS10 plays a critical role in neuroimmune interactions through negative regulation of NF-kB signaling in microglia and interaction with the PKA/CREB pathway in dopaminergic neurons (Lee, et al., 2012, Lee, et al., 2011, Lee, et al., 2008). In previous studies, global loss of RGS10 in mice results in chronic microgliosis and loss of dopaminergic neurons in response to chronic peripheral administration of LPS (Lee, et al., 2008). Given this *in vivo* phenotype and because aging is the strongest risk factor for neurodegenerative disease (Hindle, 2010, van Lookeren Campagne, et al., 2014), we sought to understand the role of RGS10 in DA neurons and immune cells in the context of aging. Loss of RGS10 does not significantly alter the distribution of peripheral immune cell subsets or dopaminergic neuron number in young mice (Fig 2, 5–7). In the brain, an increase in CD8+ T cell and granulocyte populations and a relative decrease in level of monocyte/microglia populations was seen in young RGS10-null mice (Fig 2C). With age, RGS10 expression increases in B cells, monocytes, and granulocytes while decreasing in Iba1+ brain cells (Fig 1). As suggested from the dichotomous change in RGS10 expression between the periphery and brain in specific immune cells with age, we see a difference in the timing of dysregulation of the frequency and number of immune cells in RGS10-null mice between the periphery and the brain. We observed decreased frequencies of CD4+ T cells and B cells in the peripheral blood, increased frequency of peripheral blood monocytes, and decreased number of CD4+ T cells and monocytes/macrophages in the spleen (Fig 3). RGS10 seems to play a critical role in the regulation of immune cell profiles during aging. In young mice, loss of RGS10 alters the immune cell repertoire in the CNS while leaving the peripheral immune cell repertoire largely unaltered. This pattern is reversed in aged mice just as the level of RGS10 expression becomes reversed between the periphery and CNS. These changes may suggest that RGS10 may be important for the maintenance of immune cells at different times throughout the lifespan in different compartments. The changes seen in T cell populations, in which RGS10 expression does not increase with age, may be compensatory in nature to changes in number and frequency other immune cell types. While there is no dysregulation in immune cell populations in the brains of aged RGS10-null mice, we observed an absence of increased levels of IL-6 in the CSF relative to WT mice. IL-6 is known to play an important role as a proinflammatory signal by inducing activation of immune cells and of hematopoeisis, production of acute phase reactants, and recruitment of immune cells to sites of inflammation (Tanaka, et al., 2014). It remains to be determined whether the loss of dynamics in IL-6 in CSF of aged RGS10-null mice is in response to dysregulated immunity in the CNS (as seen in young mice) or a consequence of dysregulation of immune cell populations in the periphery in aged RGS10-null mice. In summary, loss of RGS10 significantly impacts the immune cell repertoire of the young mouse brain and the aged mouse peripheral immune system.

In contrast, RGS10 does not seem to play a critical role in modulating the function of nigrostriatal dopaminergic neurons in aging as one would predict due to their sensitivity to peripheral inflammation in the RGS10-null mouse. RGS10 levels are not altered in the

ventral midbrain or striatum with age (Fig 5). Furthermore, proteins that are critical for dopaminergic neuron function are not altered by aging (Fig 6). Finally, nigrostriatal dopamine metabolism is not altered in an RGS10 dependent manner in mice (Fig 7). Taken together, these findings implicate RGS10 in regulation of immune cell populations in different compartments at different points of the lifespan rather than in dopaminergic neuron function. This dysregulated immune repertoire at different points in the lifespan is likely to indirectly affect neuron function and survival of dopaminergic and perhaps other neuronal populations and may in part explain the phenotypes that are seen in RGS10-null mice and the human disease association with ARM.

In immune cells, RGS10 has been implicated in chemokine, SHP-1, NF-kB, and macrophage M1/M2 activation pathways (Garcia-Bernal, et al., 2011, Lee, et al., 2012, Lee, et al., 2013, Ma, et al., 2012). RGS10 expression increased with age in B cells, granulocytes and monocytes while decreasing in microglia and the homeostatic frequency and number of these immune cell subsets were altered in RGS10-null mice. These findings suggest that RGS10 could be playing important regulatory functions in B cells, granulocytes, microglia and monocytes at different points in the lifespan. Given that CD4+ T cell frequency and number is altered in aged RGS10-null mice, RGS10 may also be playing a homeostatic role independent of changes in expression level in CD4+ T cells with age or these changes could be compensatory in response to changes in B cell and monocyte populations. Granulocyte expression of RGS10 increases with age but granulocyte populations were only altered in the brains of young RGS10-null mice. RGS10's roles in cellular activation in monocytes/macrophages (Lee, et al., 2013) and chemotaxis in T cells (Garcia-Bernal, et al., 2011) provide clues that activation signals and homing to lymphoid organs may be altered in RGS10-null animals that leads to altered distribution of immune cell subsets throughout the lifespan. Lack of an increase in IL-6 in the CSF of aged RGS10-null mice further suggests that dysregulated immune cell recruitment or activation may underlie observed changes. Future studies on RGS10 in aging should explore the precise immune-related mechanisms that drive the dyresgulation of immune cell population profiles.

One subtle but important point in this study is that we do not see increased levels of microglia/monocytes in the CNS of RGS10-null mice on a pure genetic background unlike previously reported for RGS10-null mice on a mixed genetic background (Lee, et al., 2008). Specifically, the first studies where chronic microgliosis was observed in RGS10-null mice was performed on mice of mixed genetic background (129/C57/BL6). All other subsequent studies from our group including the studies reported herein were performed on RGS10-null mice on a pure genetic background (C57/BL6). Unsurprisingly, genetic background and environment can have variable impact on phenotype. While we do not see chronic microgliosis on the pure background strain of RGS10-null mice, there is robust and reproducible *in vivo* immune dyregulation and *ex vivo* studies of microglia/macrophages support this conclusion (Lee, et al., 2012, Lee, et al., 2013, Lee, et al., 2011).

Overall, our data indicates that RGS10 has a role in modulating the regulation of immune cells throughout lifespan. Further understanding of the precise role of RGS10 in these immune cell populations will enhance our understanding of how dysregulated immune processes may increase the risk for age-related neurodegenerative disease. Specifically,

understanding the role of altered immune function will be important for developing novel therapies for neurodegenerative disease that show a strong inflammatory component such as Parkinson's disease and age-related maculopathy (Tansey and Goldberg, 2010, van Lookeren Campagne, et al., 2014). The role of RGS10 in human disease has not been thoroughly assessed but age-related maculopathy pathology demonstrates significant microglial activation (Buschini, et al., 2011). Interestingly, RGS10 expression in the mouse cornea increases with age but this change in expression has not be contextualized in human disease (Wu, et al., 2008). Extended immunophenotyping studies of human peripheral blood and post-mortem brains are warranted to elucidate whether altered expression of RGS10 in immune cells is detectable in age-related diseases characterized by inflammation such as age-related maculopathy and neurodegenerative diseases like Parkinson's disease.

Acknowledgments

We thank members of the Tansey lab for useful discussions. This work was supported by a grant from the Emory University Research Committee (URC) (J.K.L.), fellowship award K12GM000680 from the Emory University Fellowships in Research and Science Teaching Program's Institutional and Academic Career Development Award (C.P.R.), and grant R01NS072467 (M.G.T.) from the NINDS at the National Institutes of Health.

References

Alemany R, Perona JS, Sanchez-Dominguez JM, Montero E, Canizares J, Bressani R, Escriba PV, Ruiz-Gutierrez V. G protein-coupled receptor systems and their lipid environment in health disorders during aging. Biochimica et biophysica acta. 2007; 1768(4):964–75.10.1016/j.bbamem.2006.09.024 [PubMed: 17070497]

Berman DM, Wilkie TM, Gilman AG. GAIP and RGS4 are GTPase-activating proteins for the Gi subfamily of G protein alpha subunits. Cell. 1996; 86(3):445–52. [PubMed: 8756726]

Buschini E, Piras A, Nuzzi R, Vercelli A. Age related macular degeneration and drusen: neuroinflammation in the retina. Progress in neurobiology. 2011; 95(1):14–25.10.1016/j.pneurobio.2011.05.011 [PubMed: 21740956]

Frank-Cannon TC, Tran T, Ruhn KA, Martinez TN, Hong J, Marvin M, Hartley M, Trevino I, O'Brien DE, Casey B, Goldberg MS, Tansey MG. Parkin deficiency increases vulnerability to inflammation-related nigral degeneration. J Neurosci. 2008; 28(43):10825–34.10.1523/JNEUROSCI.3001-08.2008 [PubMed: 18945890]

Fulop T Jr, Barabas G, Varga Z, Csongor J, Hauck M, Szucs S, Seres I, Mohacsi A, Kekessy D, Despont JP, et al. Transmembrane signaling changes with aging. Ann N Y Acad Sci. 1992; 673:165–71. [PubMed: 1485715]

Garcia-Bernal D, Dios-Esponera A, Sotillo-Mallo E, Garcia-Verdugo R, Arellano-Sanchez N, Teixido J. RGS10 restricts upregulation by chemokines of T cell adhesion mediated by alpha4beta1 and alphaLbeta2 integrins. Journal of immunology. 2011; 187(3):1264–72.10.4049/jimmunol.1002960jimmunol.1002960

Gold SJ, Ni YG, Dohlman HG, Nestler EJ. Regulators of G-protein signaling (RGS) proteins: region-specific expression of nine subtypes in rat brain. J Neurosci. 1997; 17(20):8024–37. [PubMed: 9315921]

Hindle JV. Ageing, neurodegeneration and Parkinson's disease. Age and ageing. 2010; 39(2):156–61.10.1093/ageing/afp223 [PubMed: 20051606]

Hishimoto A, Shirakawa O, Nishiguchi N, Aoyama S, Ono H, Hashimoto T, Maeda K. Novel missense polymorphism in the regulator of G-protein signaling 10 gene: analysis of association with schizophrenia. Psychiatry and clinical neurosciences. 2004; 58(5):579–81.10.1111/j.1440-1819.2004.01303.x [PubMed: 15482592]

Hunt TW, Fields TA, Casey PJ, Peralta EG. RGS10 is a selective activator of G alpha i GTPase activity. Nature. 1996; 383(6596):175–7. [PubMed: 8774883]

Jakobsdottir J, Conley YP, Weeks DE, Mah TS, Ferrell RE, Gorin MB. Susceptibility genes for age-related maculopathy on chromosome 10q26. Am J Hum Genet. 2005; 77(3):389–407. S0002-9297(07)63020-1 [pii]. 10.1086/444437 [PubMed: 16080115]

Joseph JA, Cutler R, Roth GS. Changes in G protein-mediated signal transduction in aging and Alzheimer's disease. Annals of the New York Academy of Sciences. 1993; 695:42–5. [PubMed: 8239310]

Lee JK, Chung J, Druey KM, Tansey MG. RGS10 exerts a neuroprotective role through the PKA/c-AMP response-element (CREB) pathway in dopaminergic neuron-like cells. Journal of neurochemistry. 2012; 122(2):333–43.10.1111/j.1471-4159.2012.07780.x [PubMed: 22564151]

Lee JK, Chung J, Kannarkat GT, Tansey MG. Critical role of regulator G-protein signaling 10 (RGS10) in modulating macrophage M1/M2 activation. PloS one. 2013; 8(11):e81785.10.1371/journal.pone.0081785 [PubMed: 24278459]

Lee JK, Chung J, McAlpine FE, Tansey MG. Regulator of G-Protein Signaling-10 Negatively Regulates NF-{kappa}B in Microglia and Neuroprotects Dopaminergic Neurons in Hemiparkinsonian Rats. J Neurosci. 2011; 31(33):11879–88. 31/33/11879 [pii]. 10.1523/JNEUROSCI.1002-11.2011 [PubMed: 21849548]

Lee JK, McCoy MK, Harms AS, Ruhn KA, Gold SJ, Tansey MG. Regulator of G-protein signaling 10 promotes dopaminergic neuron survival via regulation of the microglial inflammatory response. J Neurosci. 2008; 28(34):8517–28. [PubMed: 18716210]

Lee JK, Tansey MG. Microglia isolation from adult mouse brain. Methods Mol Biol. 2013; 1041:17–23.10.1007/978-1-62703-520-0_3 [PubMed: 23813365]

Ma P, Cierniewska A, Signarvic R, Cieslak M, Kong H, Sinnamon AJ, Neubig RR, Newman DK, Stalker TJ, Brass LF. A newly identified complex of spinophilin and the tyrosine phosphatase, SHP-1, modulates platelet activation by regulating G protein-dependent signaling. Blood. 2012; 119(8):1935–45.10.1182/blood-2011-10-387910 [PubMed: 22210881]

Mato S, Pazos A. Influence of age, postmortem delay and freezing storage period on cannabinoid receptor density and functionality in human brain. Neuropharmacology. 2004; 46(5):716–26.10.1016/j.neuropharm.2003.11.004 [PubMed: 14996549]

Neves SR, Ram PT, Iyengar R. G protein pathways. Science. 2002; 296(5573):1636–9.10.1126/science.1071550296/5573/1636 [PubMed: 12040175]

Pankratz N, Mukhopadhyay N, Huang S, Foroud T, Kirkwood SC. Identification of genes for complex disease using longitudinal phenotypes. BMC genetics. 2003; 4(Suppl 1):S58.10.1186/1471-2156-4-S1-S58 [PubMed: 14975126]

Pascual J, del Arco C, Gonzalez AM, Diaz A, del Olmo E, Pazos A. Regionally specific age-dependent decline in alpha 2-adrenoceptors: an autoradiographic study in human brain. Neuroscience letters. 1991; 133(2):279–83. [PubMed: 1687760]

Reitz C, Mayeux R. Alzheimer disease: Epidemiology, diagnostic criteria, risk factors and biomarkers. Biochemical pharmacology. 201410.1016/j.bcp.2013.12.024

Ross EM, Wilkie TM. GTPase-activating proteins for heterotrimeric G proteins: regulators of G protein signaling (RGS) and RGS-like proteins. Annual review of biochemistry. 2000; 69:795–827.

Sastre M, Guimon J, Garcia-Sevilla JA. Relationships between beta- and alpha2-adrenoceptors and G coupling proteins in the human brain: effects of age and suicide. Brain research. 2001; 898(2):242–55. [PubMed: 11306010]

Schmidt S, Hauser MA, Scott WK, Postel EA, Agarwal A, Gallins P, Wong F, Chen YS, Spencer K, Schnetz-Boutaud N, Haines JL, Pericak-Vance MA. Cigarette smoking strongly modifies the association of LOC387715 and age-related macular degeneration. Am J Hum Genet. 2006; 78(5):852–64. S0002-9297(07)63818-X [pii]. 10.1086/503822 [PubMed: 16642439]

Shepherd KR, Lee ES, Schmued L, Jiao Y, Ali SF, Oriaku ET, Lamango NS, Soliman KF, Charlton CG. The potentiating effects of 1-methyl-4-phenyl-1,2,3,6-tetrahydropyridine (MPTP) on paraquat-induced neurochemical and behavioral changes in mice. Pharmacology, biochemistry, and behavior. 2006; 83(3):349–59.10.1016/j.pbb.2006.02.013

Siderovski DP, Diverse-Pierluissi M, De Vries L. The GoLoco motif: a Galphai/o binding motif and potential guanine-nucleotide exchange factor. Trends in biochemical sciences. 1999; 24(9):340–1. [PubMed: 10470031]

Sierra DA, Gilbert DJ, Householder D, Grishin NV, Yu K, Ukidwe P, Barker SA, He W, Wensel TG, Otero G, Brown G, Copeland NG, Jenkins NA, Wilkie TM. Evolution of the regulators of G-protein signaling multigene family in mouse and human. Genomics. 2002; 79(2):177–85. [PubMed: 11829488]

Tanaka T, Narazaki M, Kishimoto T. IL-6 in Inflammation, Immunity, and Disease. Cold Spring Harbor perspectives in biology. 2014; 6(10)10.1101/cshperspect.a016295

Tansey MG, Goldberg MS. Neuroinflammation in Parkinson's disease: its role in neuronal death and implications for therapeutic intervention. Neurobiology of disease. 2010; 37(3):510–8.10.1016/j.nbd.2009.11.004 [PubMed: 19913097]

van Lookeren Campagne M, LeCouter J, Yaspan BL, Ye W. Mechanisms of age-related macular degeneration and therapeutic opportunities. The Journal of pathology. 2014; 232(2):151–64.10.1002/path.4266 [PubMed: 24105633]

Wu F, Lee S, Schumacher M, Jun A, Chakravarti S. Differential gene expression patterns of the developing and adult mouse cornea compared to the lens and tendon. Experimental eye research. 2008; 87(3):214–25.10.1016/j.exer.2008.06.001 [PubMed: 18582462]

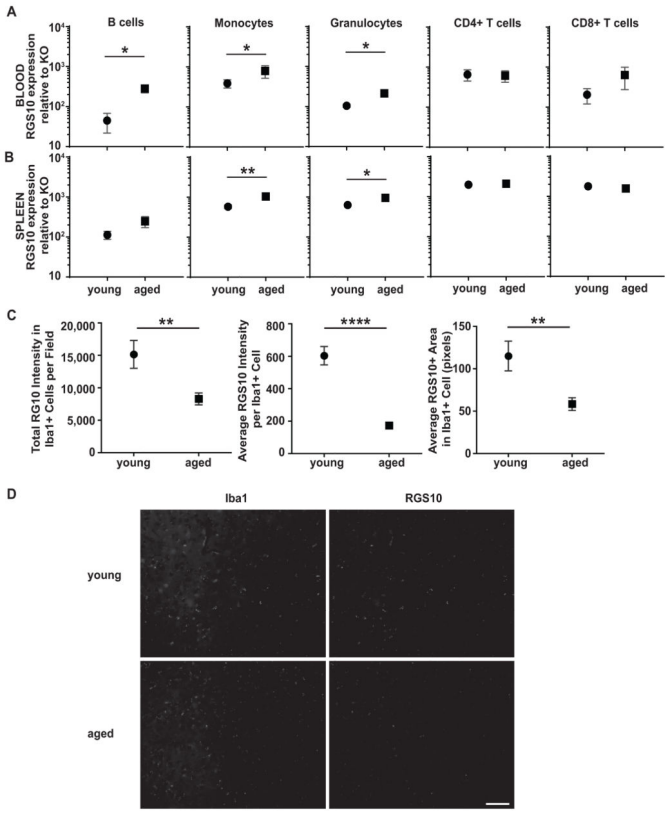

Figure 1. RGS10 expression increases in peripheral B cells, monocytes/macrophages, and granulocytes and decreases in Iba1+ cells in the brain with age

RGS10 expression was measured by intracellular staining for flow cytometry in B cells, monocytes/macrophages, granulocytes, and T cells from **A)** peripheral blood and **B)** spleens of young (circles) and aged (squares) mice, n = 4–5/group. **C)** Total RGS10 intensity in Iba1+ cells and average RGS10 intensity and area per Iba1+ cell in 20 fields per mouse (n=3 per group). **D)** Representative images of RGS10 and Iba1 staining from brains of young and old mice. Data are plotted as mean +/− standard error of the mean (SEM) for each group. P-values are indicated for two-tailed t-test: * $p < 0.05$, ** $p < 0.01$, **** $p < 0.001$.

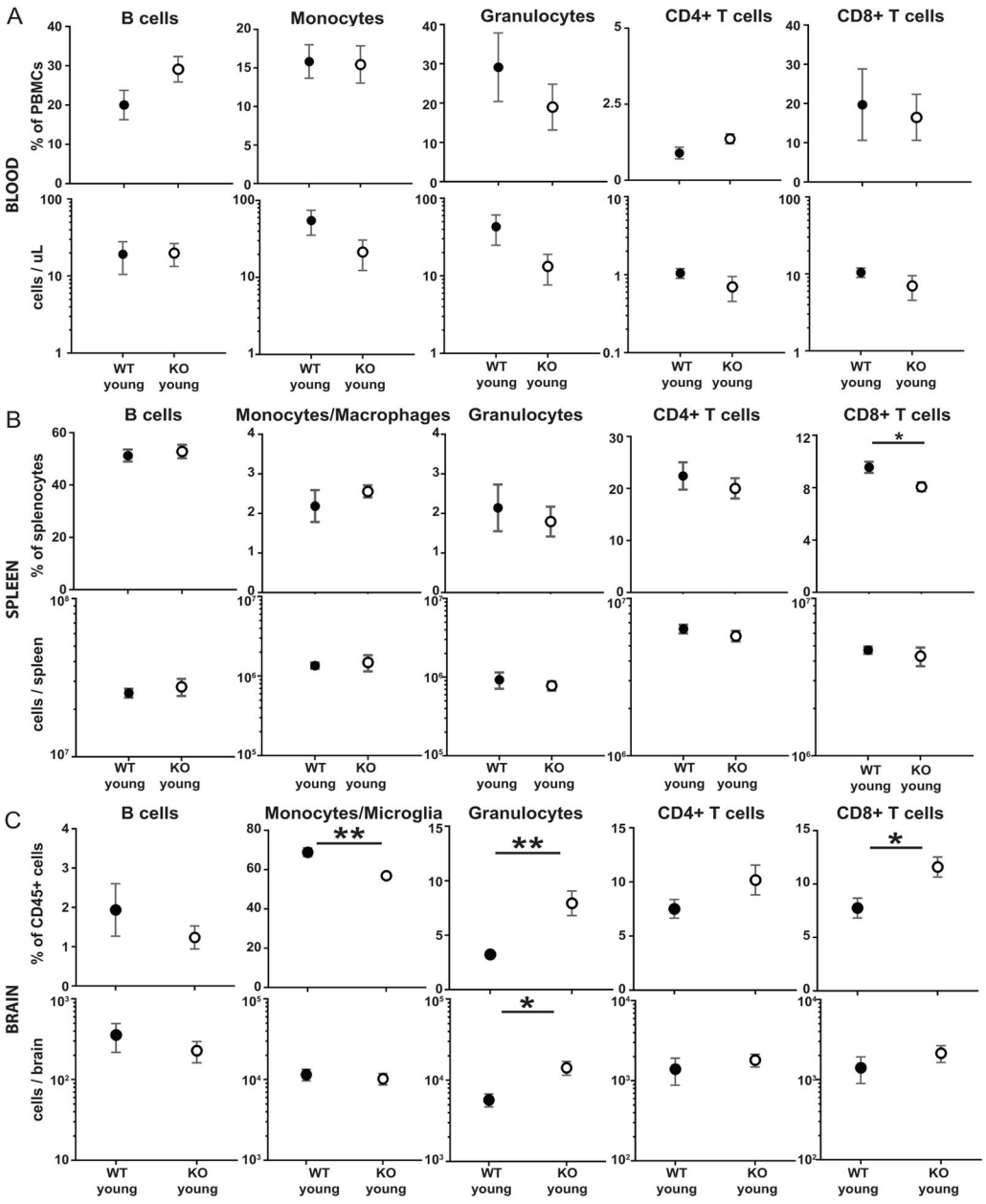

Figure 2. Loss of RGS10 alters the immune cell repertoire in the brain but has little effect on immune cell frequency and number in the periphery of young mice

Immune cell frequency and number was measured by flow cytometry in **A)** peripheral blood, **B)** spleens, and **C)** brains of young WT (black) and RGS10-null (white) mice, n = 7–9 per group. Data are plotted as mean +/− SEM for each group. P-values are indicated for two-tailed t-test: * $p < 0.05$.

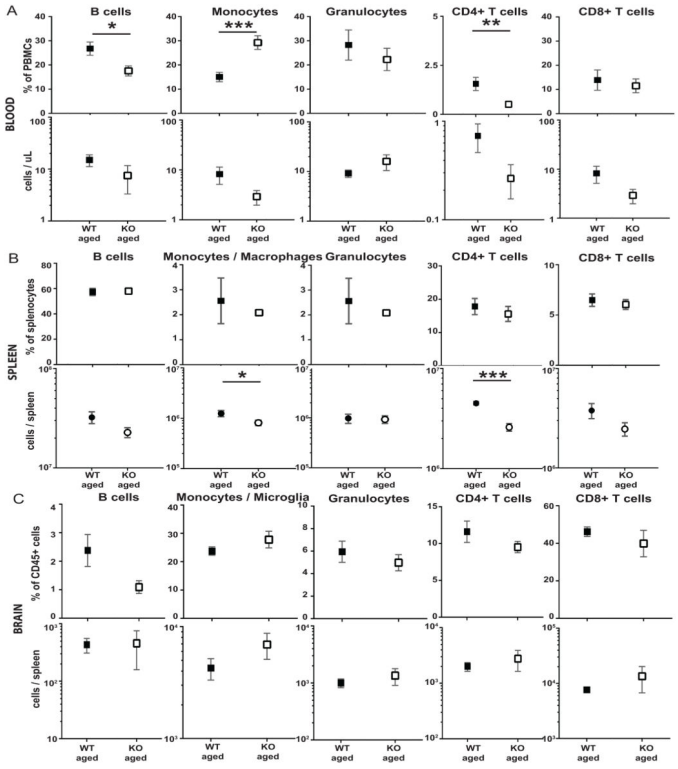

Figure 3. Loss of RGS10 alters B cell, monocyte/macrophage, and CD4+ T cell frequency and number in the periphery but not in the brain of aged mice

Immune cell frequency and number was measured by flow cytometry in **A)** peripheral blood, **B)** spleens, and **C)** brains of aged WT (black) and RGS10-null (white) mice, n = 10–13 per group. Data are plotted as mean +/− SEM for each group. P-values are indicated for two-tailed t-test: * $p < 0.05$, ** $p < 0.01$, *** $p < 0.001$.

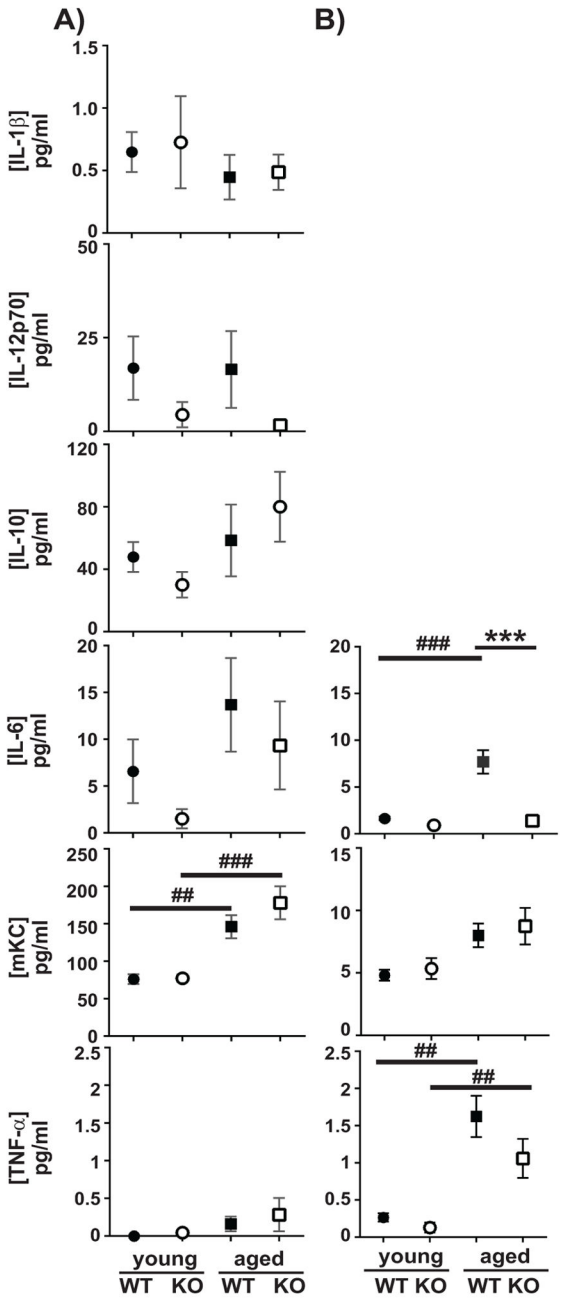

Figure 4. Loss of RGS10 does not alter serum cytokine levels but decreases IL-6 levels in the CSF in aged mice

Cytokine levels in **A)** serum and **B)** CSF from young (circles) and aged (squares) WT (black) or RGS10-null (white) mice were measured using 7-plex MesoScale Discovery Assay Kit. Serum was collected from n=9–10 mice/group and data are plotted as mean +/− SEM for each group. CSF was pooled within groups (n = 3 pools of 3–4 mice in each group). Therefore, pooled samples from 9–12 animals were analyzed. P-values are indicated for one-way ANOVA with post-hoc Holm-Sidak test. *** $p < 0.001$ for genotype-specific changes and ## $p < 0.01$, ### $p < 0.001$ for age-specific changes.

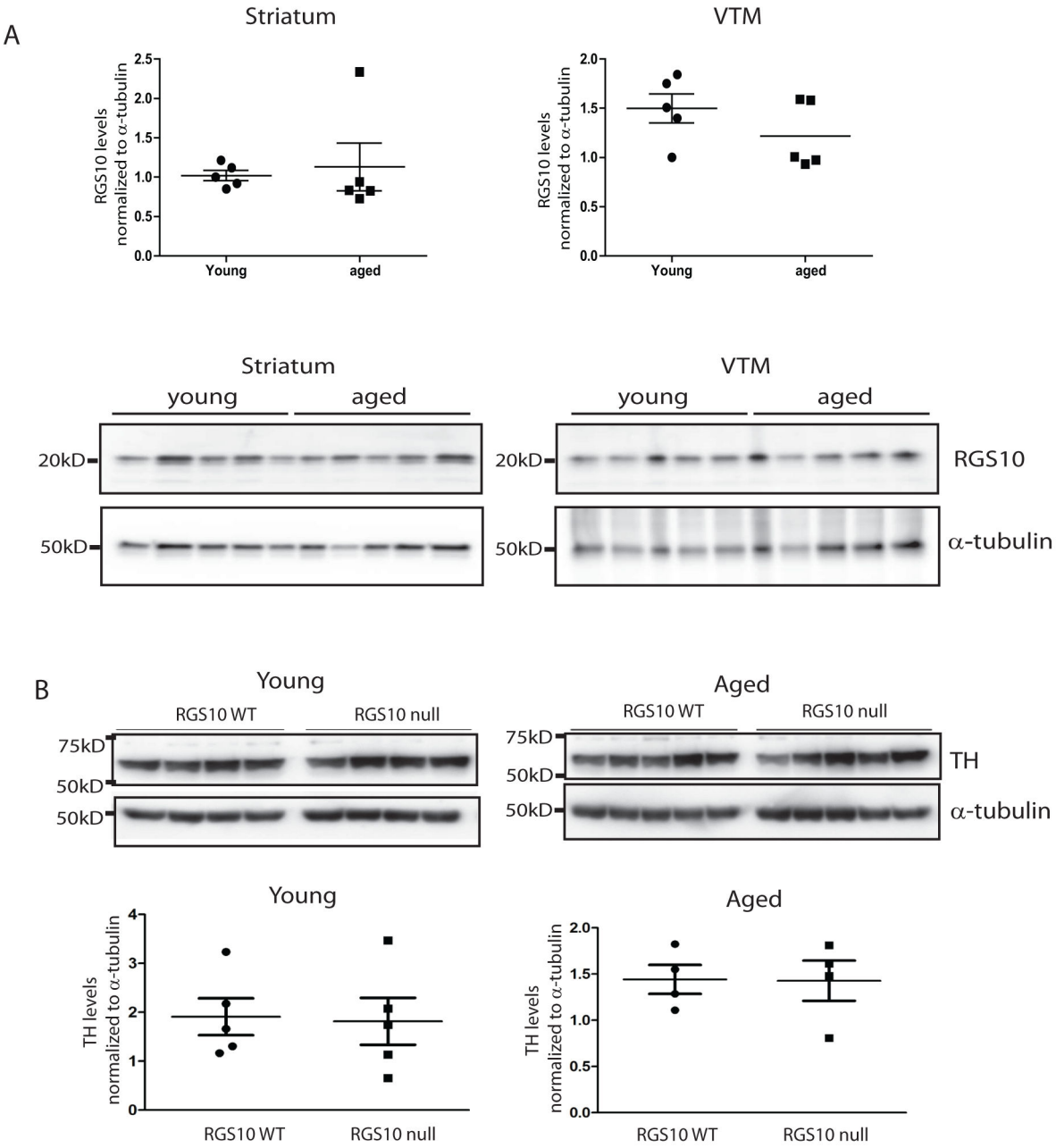

Figure 5. RGS10 expression does not change with age in the ventral midbrain or striatum and does not alter TH expression in the ventral midbrain in young or aged mice

A) Soluble protein lysates from ventral midbrain (VMB) or striatal tissues of young and aged RGS10 WT animals were analyzed for the levels of RGS10 protein expression. B) Total protein lysates were extracted from VMB tissues of young and aged animals and were assessed by immunoblot for the levels of TH and α-tubulin. Membranes were also probed with mouse monoclonal α-tubulin antibody to assess protein loading. RGS10 expression was quantified by densitometry and normalized to α-tubulin expression. Data were plotted as a scatter with each point representing an individual animal and mean +/− SEM for each

group. Two-tailed student's t-test was used to test for significance. No significant differences were noted.

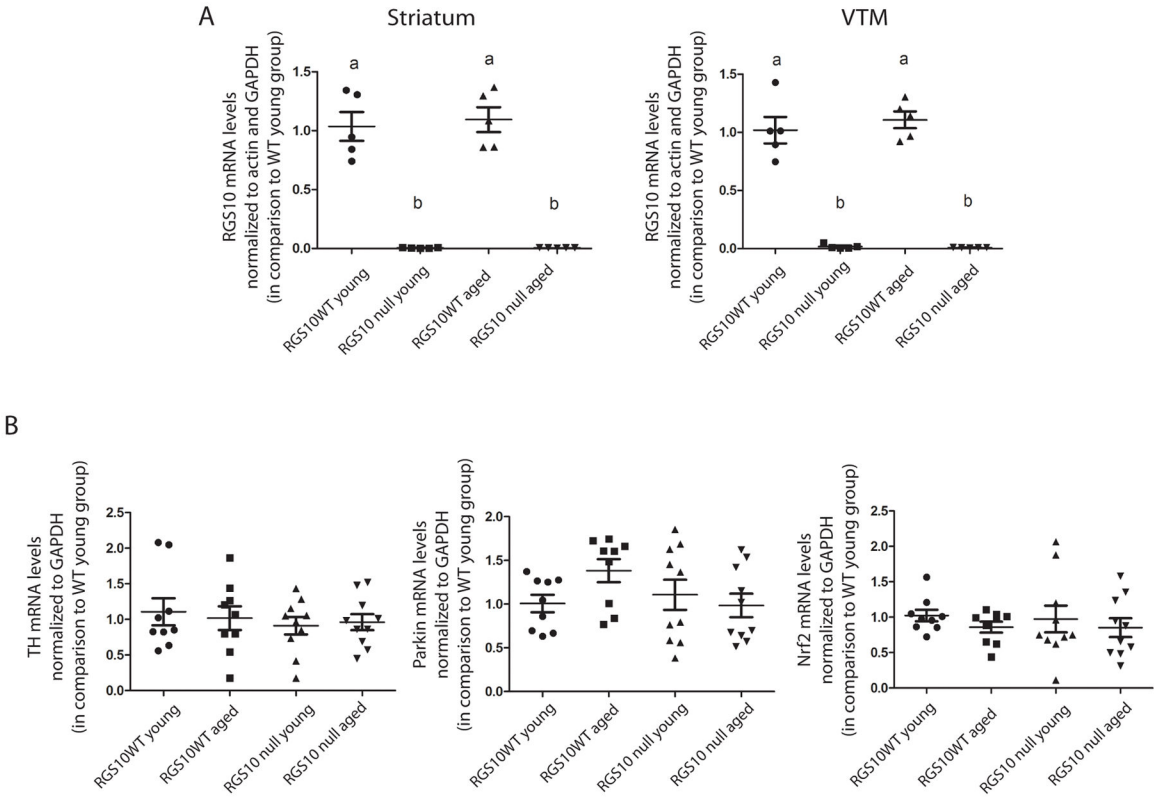

Figure 6. Loss of RGS10 does not alter mRNA expression for TH, Parkin, or Nrf2 in the ventral midbrain

A) Total RNA was extracted from ventral midbrain (VMB) or striatal tissues of young or aged RGS10 WT or RGS10-null animals and was analyzed by qRT-PCR. The resulting Ct values were analyzed by the ΔΔCt method using the RGS10 young wild-type group as the control group and the mean of Ct values for actin and GAPDH. Experiments were performed in triplicate. Data were plotted as a scatter with each point representing an individual animal and mean +/− SEM for each group. Data was analyzed by one-way ANOVA followed by bonferroni's post-hoc test. Columns with matching lower case letters are not statistically different. $p<0.0001$ **B**) VMB tissues from young and aged animals were analyzed by QPCR using primers directed against murine TH, Parkin, Nrf2, and GAPDH genes. For each animal, the Ct values for TH, Parkin, and Nrf2 were normalized to the Ct values for GAPDH. The data was graph and analyzed as previously described. No statistically significant differences were observed.

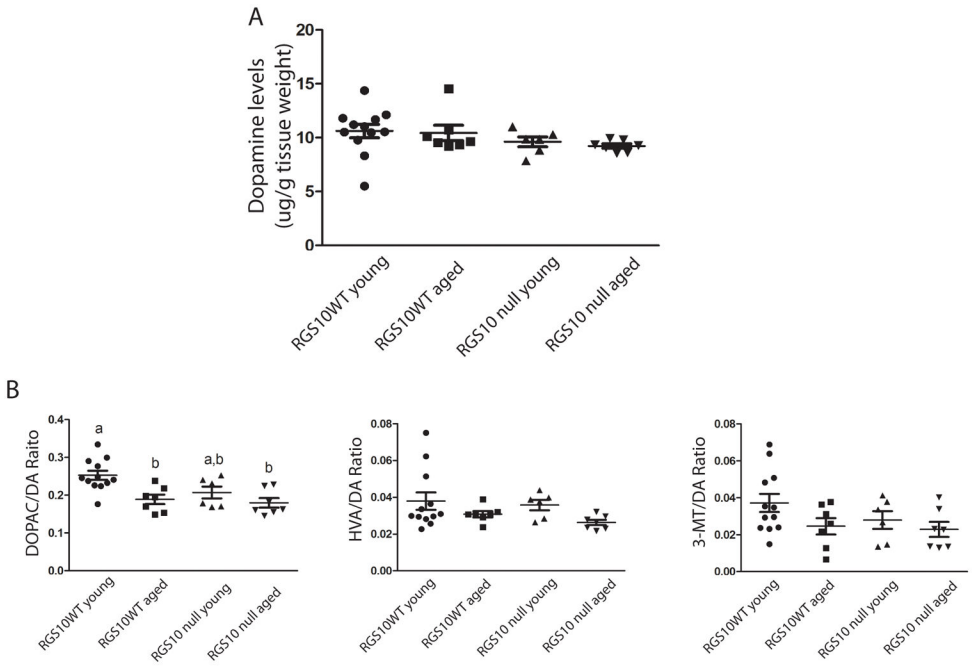

Figure 7. The levels of nigrostriatal DA and metabolites are independent of RGS10 expression

Coronal sections of striatum (2mm) were dissected from young and aged RGS10 WT and null mice (n = 4 per age group, per genotype). Tissue was weighed and homogenized in 10 volumes of ice-cold catechol extraction buffer. Following sedimentation, the resulting supernatants were filtered and filtrates were analyzed using reverse-phase ion pairing ultra-high pressure liquid chromatography combined with an electrochemical detector under isocratic conditions. Analyte levels were normalized to tissue weight. In **A**), the micrograms of dopamine (DA) per gram of tissue are shown for the respective animals groups. In the scatter plots, the horizontal line denotes the mean of the indicated group. The error bars indicate the standard error of the mean. Each point represents a distinct animal. The graph was analyzed by one-way ANOVA and Bonferroni's post hoc test. No significant differences were observed. **B**) The ratio of the levels of DA metabolites 3–4-dihydroxphenylacetic acid ("DOPAC"), homovanillic acid ("HVA"), or 3-methoxytyramine ("3-MT") to DA were calculated for each animal and graphed. Graphs were analyzed by one-way ANOVA and Bonferroni's post hoc test. Columns with matching letters are not statistically different. $p<0.01$